

TiO₂ Nanocrystals Grown on Graphene as Advanced Photocatalytic Hybrid Materials

Yongye Liang[§], Hailiang Wang[§], Hernan Sanchez Casalongue, Zhuo Chen, and Hongjie Dai (✉)

Department of Chemistry and Laboratory for Advanced Materials, Stanford University, Stanford, CA 94305, USA

Received: 18 July 2010 / Revised: 11 August 2010 / Accepted: 12 August 2010

© The Author(s) 2010. This article is published with open access at Springerlink.com

ABSTRACT

A graphene/TiO₂ nanocrystals hybrid has been successfully prepared by directly growing TiO₂ nanocrystals on graphene oxide (GO) sheets. The direct growth of the nanocrystals on GO sheets was achieved by a two-step method, in which TiO₂ was first coated on GO sheets by hydrolysis and crystallized into anatase nanocrystals by hydrothermal treatment in the second step. Slow hydrolysis induced by the use of EtOH/H₂O mixed solvent and addition of H₂SO₄ facilitates the selective growth of TiO₂ on GO and suppresses growth of free TiO₂ in solution. The method offers easy access to the GO/TiO₂ nanocrystals hybrid with a uniform coating and strong interactions between TiO₂ and the underlying GO sheets. The strong coupling gives advanced hybrid materials with various applications including photocatalysis. The prepared graphene/TiO₂ nanocrystals hybrid has superior photocatalytic activity to other TiO₂ materials in the degradation of rhodamine B, showing an impressive three-fold photocatalytic enhancement over P25. It is expected that the hybrid material could also be promising for various other applications including lithium ion batteries, where strong electrical coupling to TiO₂ nanoparticles is essential.

KEYWORDS

Graphene, titanium oxide, photocatalyst, hydrolysis

Its interesting electrical and mechanical properties, and high surface area make graphene a novel substrate for forming hybrid structures with a variety of nanomaterials [1–3]. Graphene hybrids with metal oxides, metals and polymers have been developed recently for various applications [4–6]. Nanocrystal growth on graphene sheets is an important approach to produce nanohybrids, since controlled nucleation and growth affords optimal chemical interactions and bonding between nanocrystals and graphene sheets, leading to very strong electrical and mechanical coupling within

the hybrid. Several methods have been proposed to form nanocrystals on graphene sheets, such as electrochemical deposition [7], sol–gel process [8] and gas phase deposition [9, 10]. Recently, we developed a controlled, two-step solution phase synthesis of nanocrystals of Ni, Fe, and Co hydroxides or oxides on graphene sheets, which is highly selective in that there is no growth of free nanocrystals in solution [1]. We demonstrated the excellent performance of nickel hydroxide nanoplates grown on graphene for electrochemical pseudocapacitive energy storage, utilizing

[§] These authors contributed equally.

Address correspondence to hdai@stanford.edu



the high electrical conductivity of graphene [4].

Here we present a two-step, direct synthesis of TiO_2 nanocrystals on graphene oxide (GO) and the photocatalytic properties of the resulting hybrid material. Due to its low cost, high stability and efficient photoactivity, TiO_2 has been widely used for photoelectrochemical and photocatalytic applications [11]. Several graphene/ TiO_2 composites have been reported recently for use in lithium ion batteries [12], photocatalysis [13], and dye sensitized solar cells [14], using either surfactant-assisted growth or simple physical mixing of pre-synthesized TiO_2 particles and graphene. Here we achieve surfactant-free growth of TiO_2 nanocrystals on graphene with optimal TiO_2 -graphene coupling. By limiting the rate of hydrolysis, we obtain a high degree of control which confines TiO_2 nanocrystal growth selectively on the graphene oxide sheets, without any growth of free TiO_2 in solution. The resulting hybrid material showed superior photocatalytic degradation of rhodamine B and methylene blue relative to a variety of other TiO_2 materials.

GO prepared by a modified Hummers' method [15–18] was used as a substrate for TiO_2 growth giving TiO_2/GO hybrids (containing ~10% GO by mass). Details are given in the Electronic Supplementary Material (ESM). The functional groups on GO provide reactive and anchoring sites for nucleation and growth of nanomaterials (Fig. 1) [1]. In the first reaction step, fine particles of almost amorphous TiO_2 (see the XRD

pattern in Fig. S-1 in the ESM) were coated on GO sheets by hydrolysis of $\text{Ti}(\text{BuO})_4$ at 80 °C by addition of H_2SO_4 in a $\text{EtOH}/\text{H}_2\text{O}$ (15/1 by volume) mixed solvent, designed to slow down the hydrolysis reaction. This led to selective growth of TiO_2 on GO (Fig. 1(b)) without any obvious growth of free TiO_2 particles in solution. Rapid hydrolysis occurred when water alone was used as the solvent, or without the addition of H_2SO_4 ; in these cases growth of TiO_2 particles in solution, not associated with GO, was observed (see Fig. S-2 in the ESM). In the second step, we carried out a hydrothermal treatment of the amorphous TiO_2/GO at 200 °C in a mixed water/DMF solvent (Fig. 1(c)), which led to crystallization of the coating material on GO giving anatase nanocrystals (Figs. 2(b)–2(d)).

We used water/DMF (50/1 by volume) mixed solvent in the second step since DMF was found to facilitate dispersion of the graphene sheets and reduce aggregation, as shown by the higher surface area (190 m^2/g) for the resulting hybrid compared with that of the material (134 m^2/g) obtained in pure water. Electron microscopy images (Figs. 1(c), 2(a) and 2(b)) revealed dense TiO_2 nanocrystals densely bound to GO sheets, which were not detached even under sonication. High resolution TEM (Fig. 2(c)) showed that TiO_2 grown on GO adopts a highly crystalline anatase phase, consistent with the XRD pattern (Fig. 2(d)).

The density of TiO_2 nanocrystals coated on graphene was controlled by the feed ratio of $\text{Ti}(\text{BuO})_4/\text{GO}$,

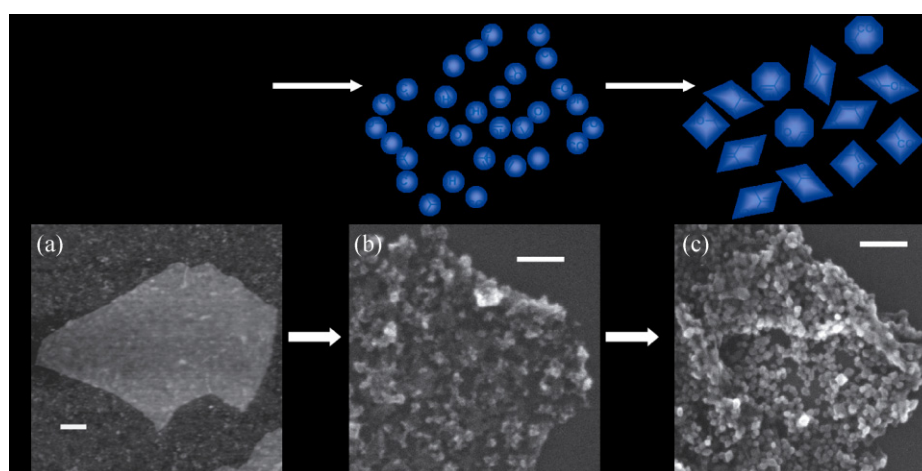


Figure 1 Synthesis of TiO_2 nanocrystals on GO sheets. Top panel: Reaction scheme: (a) AFM image of a starting GO sheet; (b) SEM image of particles grown on a GO sheet after the first hydrolysis reaction step; (c) SEM image of TiO_2 nanocrystals on GO after hydrothermal treatment in the second step. The scale bars are 100 nm

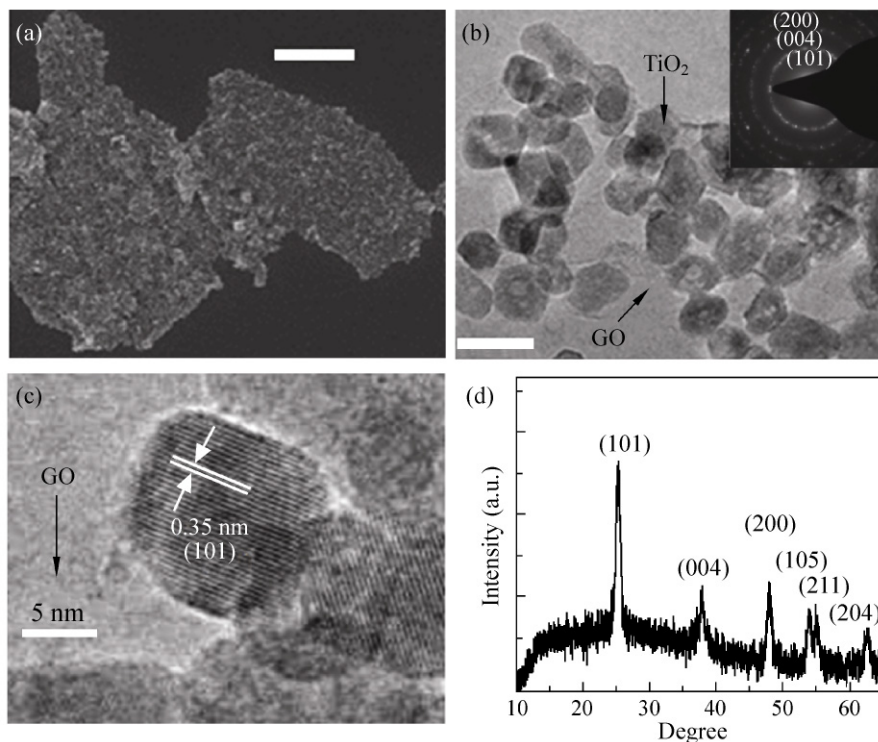


Figure 2 (a) SEM image, (b) low magnification, and (c) high magnification TEM images of TiO_2 nanocrystals grown on GO sheets. The scale bar is 400 nm for the SEM image in (a) and 20 nm for the TEM image in (b). (d) An XRD pattern of the graphene/ TiO_2 nanocrystals hybrid

increasing as the amount of $\text{Ti}(\text{BuO})_4$ increased (Fig. 3). The average size of the TiO_2 nanocrystals depended on the EtOH/water ratio in the first step, increasing from ~ 15 nm in EtOH/water (15/1) to ~ 30 nm in EtOH/water (3/1) (Fig. S-3 in the ESM). This is because the rate of the hydrolysis reaction increased with increasing water content. This was accompanied by a decrease in surface area for TiO_2/GO synthesized in EtOH/water mixtures with higher water concentrations (Table S-1 in the ESM).

TiO_2 nanocrystals directly grown on graphene appeared to exhibit strong interactions with the underlying GO sheets since sonication did not lead to their dissociation from the sheets. This strong coupling should lead to advanced hybrid materials for various applications, including photocatalysis. TiO_2 has been widely used as a photocatalytic semiconductor for decontamination of organic pollutants. A limiting factor in the rate of photocatalysis reaction is the rapid electron-hole recombination [19]. In order to increase the charge separation lifetime, carbon nanotube (CNT)- TiO_2 hybrids have been produced; these

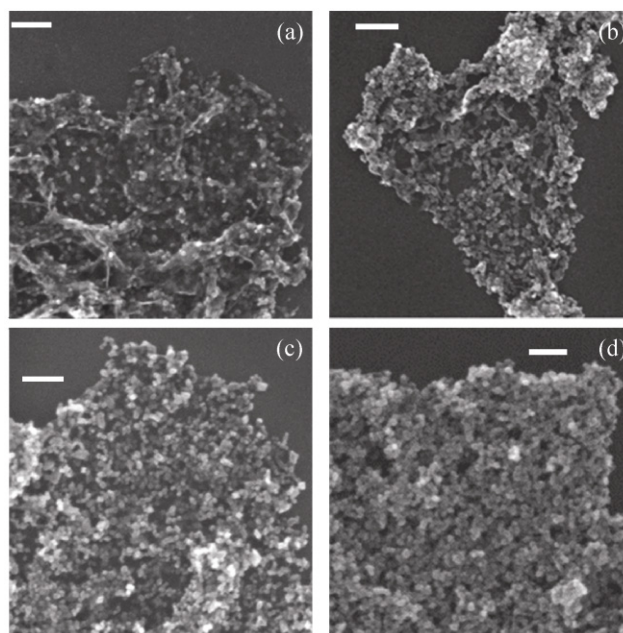


Figure 3 SEM images of graphene/ TiO_2 hybrids formed with various GO/ TiO_2 mass ratios: (a) 1:1, (b) 1:3, (c) 1:9, (d) 1:18. The scale bars are 100 nm. The TiO_2 coating density is controlled by varying the feed ratio of $\text{Ti}(\text{BuO})_4/\text{GO}$. The coating of TiO_2 nanocrystals on graphene becomes denser as the $\text{Ti}(\text{BuO})_4/\text{GO}$ feed ratio is increased

enhance the rate of photocatalysis reaction through transfer of photoexcited electrons to the CNTs [20].

We tested the photocatalytic performance of our graphene/TiO₂ nanocrystals hybrid in the photodegradation of rhodamine B under UV irradiation (Fig. 4(a)) and compared it with free TiO₂ nanocrystals synthesized by the same method in the absence of GO, and P25 (a well-known commercial TiO₂ photocatalyst). The amount of TiO₂ was kept the same in all these samples. The hybrid sample used for the photocatalytic measurements was prepared using EtOH/water = 15/1 (volume ratio) in the first step and water/DMF = 50/1 (volume ratio) in the second step with TiO₂/GO = 9/1 (mass ratio). The kinetics of the degradation reaction were fitted to a pseudo first-order reaction at low dye concentrations: $\ln(c_0/c) = kt$, where k is the apparent rate constant [21]. The average value of k for the hybrid ($k = 0.200 \text{ min}^{-1}$) was found to be ca. four times that of free TiO₂ grown in

solution ($k = 0.050 \text{ min}^{-1}$) and three times that of P25 ($k = 0.068 \text{ min}^{-1}$). We also prepared a simple mixture of P25 and GO and hydrothermally treated the mixture as reported in the literature [13]; the resulting mixture gave a value of $k = 0.090 \text{ min}^{-1}$, less than half that for our directly grown graphene/TiO₂ hybrid (Figs. 4(b) and 4(c)). The three-fold enhancement in photocatalytic activity of our hybrid over P25 is impressive, considering the low cost of GO and the highest reported enhancement factor (ca. two) for CNT–TiO₂ composites over P25 [20]. The superior photocatalytic activity of our graphene/TiO₂ hybrid was also demonstrated in the degradation of methylene blue. The average rate constant for the hybrid ($k = 0.128 \text{ min}^{-1}$) is much larger than those for P25 ($k = 0.055 \text{ min}^{-1}$) and a simple mixture of P25 and GO ($k = 0.084 \text{ min}^{-1}$) (Fig. S-4 in the ESM).

The high photocatalytic activity of our hybrid could be a result of the strong coupling between TiO₂ and GO which facilitates interfacial charge transfer (with GO as an electron acceptor) and inhibits electron–hole recombination [22]. Another possible contributing factor is that the hybrid material has a higher BET surface area (190 m²/g) than both free TiO₂ grown in solution (121 m²/g) and P25 (58 m²/g). In addition, the conjugated dye molecules could bind to large aromatic domains on GO sheets via π – π stacking, which could favor increased reactivity [19].

In conclusion, we have successfully grown TiO₂ nanocrystals on graphene with a well-controlled coating density by a two step method. This method produced a graphene/TiO₂ hybrid with strong interactions between the two components. The resulting hybrid material shows superior photocatalytic activity to other forms of TiO₂. We expect that the hybrid material could also be useful for various other applications including TiO₂-based electrodes for dye-sensitized solar cells and lithium ion batteries, where strong electrical coupling to TiO₂ nanoparticles are also important. Our method could be further extended to grow other functional materials on graphene for advanced hybrid materials.

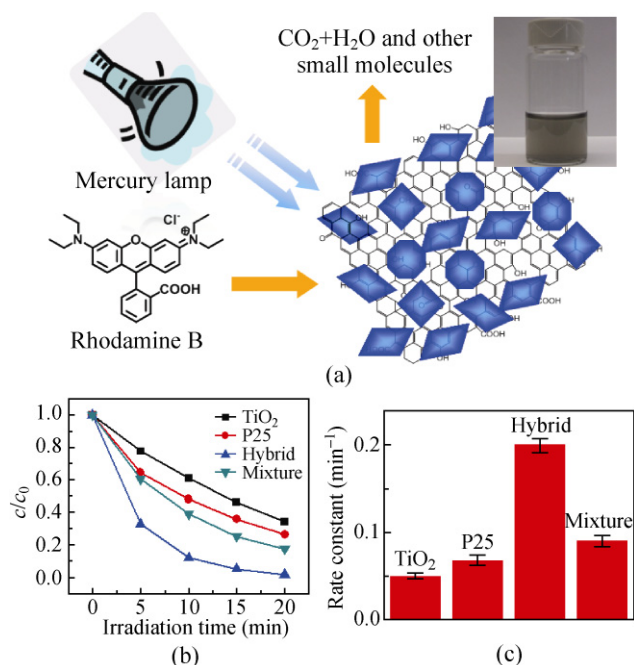


Figure 4 (a) Schematic illustration of the photodegradation of rhodamine B molecules by the graphene/TiO₂ nanocrystals hybrid under irradiation by a mercury lamp. The inset shows the solution of the graphene/TiO₂ nanocrystals hybrid. (b) Photocatalytic degradation of rhodamine B monitored as normalized concentration change versus irradiation time in the presence of free TiO₂, P25, graphene/TiO₂ nanocrystals hybrid and a graphene/TiO₂ mixture. (c) Average reaction rate constant (min⁻¹) for the photodegradation of rhodamine B with free TiO₂, P25, graphene/TiO₂ nanocrystals hybrid, and the graphene/TiO₂ mixture. The error bars are based on measurements on at least four different samples

Acknowledgements

This work was supported in part by Intel, MARCO-MSD, and ONR.

Electronic Supplementary Material: Supplementary material (details of the synthesis of the graphene/TiO₂ hybrid and additional experimental data) is available in the online version of this article at <http://dx.doi.org/10.1007/s12274-010-0033-5> and is accessible free of charge.

Open Access: This article is distributed under the terms of the Creative Commons Attribution Noncommercial License which permits any noncommercial use, distribution, and reproduction in any medium, provided the original author(s) and source are credited.

References

- [1] Wang, H. L.; Robinson, J. T.; Diankov, G.; Dai, H. J. Nanocrystal growth on graphene with various degrees of oxidation. *J. Am. Chem. Soc.* **2010**, *132*, 3270–3271.
- [2] Si, Y. C.; Samulski, E. T. Exfoliated graphene separated by platinum nanoparticles. *Chem. Mater.* **2008**, *20*, 6792–6797.
- [3] Lee, D. H.; Kim, J. E.; Han, T. H.; Hwang, J. W.; Jeon, S.; Choi, S. Y.; Hong, S. H.; Lee, W. J.; Ruoff, R. S.; Kim, S. O. Versatile carbon hybrid films composed of vertical carbon nanotubes grown on mechanically compliant graphene films. *Adv. Mater.* **2010**, *22*, 1247–1252.
- [4] Wang, H. L.; Sanchez Casalongue, H.; Liang, Y. Y.; Dai, H. J. Ni(OH)₂ nanoplates grown on graphene as advanced electrochemical pseudocapacitor materials. *J. Am. Chem. Soc.* **2010**, *132*, 7472–7477.
- [5] Yoo, E. J.; Okata, T.; Akita, T.; Kohyama, M.; Nakamura, J.; Honma, I. Enhanced electrocatalytic activity of Pt subnanoclusters on graphene nanosheet surface. *Nano Lett.* **2009**, *9*, 2255–2259.
- [6] Murugan, A. V.; Muraliganth, T.; Manthiram, A. Rapid, facile microwave-solvothermal synthesis of graphene nanosheets and their polyaniline nanocomposites for energy storage. *Chem. Mater.* **2009**, *21*, 5004–5006.
- [7] Williams, G.; Seger, B.; Kamat, P. V. TiO₂-graphene nanocomposites. UV-assisted photocatalytic reduction of graphene oxide. *ACS Nano* **2008**, *2*, 1487–1491.
- [8] Wang, D. H.; Kou, R.; Choi, D. W.; Yang, Z. G.; Nie, Z. M.; Li, J.; Saraf, L. V.; Hu, D. H.; Zhang, J. G.; Graff, G. L.; Liu, J.; Pope, M. A.; Aksay, I. A. Ternary self-assembly of ordered metal oxide-graphene nanocomposites for electrochemical energy storage. *ACS Nano*, **2010**, *4*, 1587–1595.
- [9] Wang, X. R.; Tabakman, S. M.; Dai, H. J. Atomic layer deposition of metal oxides on pristine and functionalized graphene. *J. Am. Chem. Soc.* **2008**, *130*, 8152–8153.
- [10] Lu, G. H.; Mao, S.; Park, S.; Ruoff, R. S.; Chen, J. H. Facile, noncovalent decoration of graphene oxide sheets with nanocrystals. *Nano Res.* **2009**, *2*, 192–200.
- [11] Chen, X. B.; Mao, S. S. Titanium dioxide nanomaterials: Synthesis, properties, modifications, and applications. *Chem. Rev.* **2007**, *107*, 2891–2959.
- [12] Wang, D. H.; Choi, D. W.; Li, J.; Yang, Z. G.; Nie, Z. M.; Kou, R.; Hu, D. H.; Wang, C. M.; Saraf, L. V.; Zhang, J. G.; Aksay, I. A.; Liu, J. Self-assembled TiO₂-graphene hybrid nanostructures for enhanced Li-ion insertion. *ACS Nano*, **2009**, *3*, 907–914.
- [13] Zhang, H.; Lv, X. J.; Li, Y. M.; Wang, Y.; Li, J. H. P25-graphene composite as a high performance photocatalyst. *ACS Nano* **2010**, *4*, 380–386.
- [14] Yang, N. L.; Zhai, J.; Wang, D.; Chen, Y. S.; Jiang, L. Two-dimensional graphene bridges enhanced photoinduced charge transport in dye-sensitized solar cells. *ACS Nano*, **2010**, *4*, 887–894.
- [15] Hummer, W. S.; Offeman, R. E. Preparation of graphitic oxide. *J. Am. Chem. Soc.* **1958**, *80*, 1339–1339.
- [16] Wang, H. L.; Wang, X. R.; Li, X. L.; Dai, H. J. Chemical self-assembly of graphene sheets. *Nano Res.* **2009**, *2*, 336–342.
- [17] Sun, X. M.; Liu, Z.; Welsher, K.; Robinson, J. T.; Goodwin, A.; Zoric, S.; Dai, H. J. Nano-graphene oxide for cellular imaging and drug delivery. *Nano Res.* **2008**, *1*, 203–212.
- [18] Wang, H. L.; Robinson, J. T.; Li, X. L.; Dai, H. J. Solvothermal reduction of chemically exfoliated graphene sheets. *J. Am. Chem. Soc.* **2009**, *131*, 9910–9911.
- [19] Ravelli, D.; Dondi, D.; Fagnoni, M.; Albin, A. Photocatalysis. A multi-faceted concept for green chemistry. *Chem. Soc. Rev.* **2009**, *38*, 1999–2011.
- [20] Woan, K.; Pyrgiotakis, G.; Sigmund, W. Photocatalytic carbon-nanotube-TiO₂ composites. *Adv. Mater.* **2009**, *21*, 2233–2239.
- [21] Wang, X. H.; Li, J. G.; Kamiyama, H.; Moriyoshi, Y.; Ishigaki, T. Wavelength-sensitive photocatalytic degradation of methyl orange in aqueous suspension over iron(III)-doped TiO₂ nanopowders under UV and visible light irradiation. *J. Phys. Chem. B*, **2006**, *110*, 6804–6809.
- [22] Wang, W. D.; Serp, P.; Kalck, P.; Faria, J. L. Photocatalytic degradation of phenol on MWNT and titania composite catalysts prepared by a modified sol-gel method. *Appl. Catal. B* **2005**, *56*, 305–312.

